recycling

MDPI

Article

Predicting the Properties of Construction Concrete Modified with a Nanopreparation and Containing E-Waste Plastic

Ruslan Sapinov [1,2,*], Natalya A. Kulenova [1], Marzhan A. Sadenova [1], Nikolay Charykov [1,3], Olga V. Rudenko [1], Zhanserik Shoshay [1,2] and Yegor Rakov [1]

[1] Priority Department Centre "Veritas" D. Serikbayev East Kazakhstan Technical University, 19 Serikbayev Str., Ust-Kamenogorsk 070000, Kazakhstan; nkulenova@edu.ektu.kz (N.A.K.); msadenova@edu.ektu.kz (M.A.S.); ncharykov@yandex.ru (N.C.); orudenko@edu.ektu.kz (O.V.R.); zhanserik@inbox.ru (Z.S.); riventpro@gmail.com (Y.R.)
[2] Faculty of Engineering, NJSC Toraighyrov University, Lomov Street, 64, Pavlodar 140008, Kazakhstan
[3] Department of Physical Chemistry, Saint-Petersburg State Institute of Technology, Technical University, 26, Moskovskii Prospekt, Saint-Petersburg 190013, Russia
* Correspondence: sapinov.r@teachers.tou.edu.kz

Abstract

This study addresses the pressing issue of utilising plastic from electronic waste as a filler to replace mineral sand. Currently, the use of plastic in construction concrete is limited due to a significant deterioration in the mechanical properties of modified concrete when plastic filler is added at levels exceeding 15–20%. As a result of the research, it was established that the addition of a nano-preparation—fullerene—in amounts as low as 0.001% significantly improves the mechanical properties of concrete with plastic aggregate. Replacing 50% of the mineral aggregate with plastic aggregate, combined with the addition of fullerene at a concentration of 0.01% of the mixing water mass, more than doubles the mechanical properties of the concrete compared to concrete without the nano-additive, with compressive strength increasing by 65.2%, from 16.33 MPa to 26.97 MPa. The impact strength and freeze–thaw resistance of the concrete were also significantly increased. This makes it possible to use concrete with a high plastic aggregate content of up to 50% without a significant reduction in mechanical properties. The use of machine learning and AI data processing methods such as AdaBoost and Random Forest allows for highly accurate prediction of the characteristics of the resulting materials, with a coefficient of determination (R^2) for the resulting models close to 1.

Keywords: e-waste; ABC plastic; carbon nanomaterials; concrete; compressive strength; impact strength; frost resistance

Check for updates

Academic Editor: Sha Liang

Received: 21 May 2026
Revised: 9 June 2026
Accepted: 11 June 2026
Published: 14 June 2026

Copyright: © 2026 by the authors. Licensee MDPI, Basel, Switzerland. This article is an open access article distributed under the terms and conditions of the Creative Commons Attribution (CC BY) license.

1. Introduction

The current pace of industrialisation, technological progress, and rising living standards are leading to a rapid increase in the volume of electronic waste. This category includes obsolete devices such as televisions, laptops, computers, and household appliances. The urgency of the issue of electronic waste recycling is beyond doubt. The primary focus in electronic waste recycling is on metals [1,2]. However, plastic accounts for approximately 20–30% of the total volume of electronic waste [3]. Plastic production is expected to grow exponentially in the future [4]. The slow rate at which plastic degrades creates critical environmental problems [5]. Moreover, the fragmentation of plastic leads to the formation of microplastics enriched with metals and organic compounds, which easily

penetrate living organisms, causing adverse effects [6–8]. Despite the economic feasibility, a significant portion of plastic computer equipment casings (primarily ABS plastic and impact-resistant polystyrene) still ends up in landfills. The reasons for the low economic appeal of e-waste plastics compared to metals are the technological challenges involved in separating them and the presence of various additives in them. As a result, the plastic fraction of electronic waste is often treated as a residual stream after the extraction of valuable metals and is disposed of through landfilling or open burning [9]. Studies show that the use of plastic waste as a construction material holds enormous potential for large-scale construction; however, polymers such as ABS (acrylonitrile butadiene styrene) have not yet received sufficient attention [10]. ABS plastic is the most common polymer used in the production of monitor and printer housings [11]. It has high heat resistance (up to 110 °C), cold resistance (down to −40 °C), and chemical resistance to alkalis and oils. Adding plastic to concrete is considered an environmentally friendly and cost-effective method of disposal. Previous studies have confirmed the successful use of PET flakes [12], HDPE waste [13], and PVC [14] as partial replacements for aggregates. Such modifications allow for a reduction in concrete weight and an increase in its corrosion resistance. From an environmental perspective, replacing natural sand with recycled plastic helps reduce the carbon footprint [15]. In addition, plastic aggregates improve the thermal insulation properties of buildings, thereby increasing their energy efficiency [16]. A key barrier to the widespread use of e-plastic in civil engineering is the reduction in the mechanical properties of conventional concrete when it is added [17,18]. A promising approach to addressing this issue is the use of nanomaterials such as cellulose nanofibers (CNF) [19], silicon dioxide nanoparticles (NS), calcium carbonate nanoparticles (NC) [20], and carbon nanoparticles, the effectiveness of which in concrete has been confirmed by numerous studies [21,22]. To better understand how various factors influence the mechanical properties of concrete, we plan to apply mathematical methods. Predicting the mechanical properties of concrete using a polynomial model and response surfaces (RSM) allows us to evaluate the synergistic effect of multiple factors [23]. A comparative evaluation of the obtained polynomial models was conducted using machine learning algorithms, in accordance with the methodology proposed in a study dedicated to predicting the compressive strength of concrete based on machine learning. This approach allows for a more comprehensive assessment of the accuracy of the obtained mathematical model [24].

The aim of this study is to investigate the properties of concrete containing ABS plastic derived from electronic waste and carbon-based nanomaterials, which are added to compensate for the loss of mechanical properties that occurs when standard aggregate is replaced with plastic, and to predict these properties using mathematical models and machine learning. To this end, the following tasks will be addressed:

- Prepare recycled ABS plastic from electronic waste and produce concrete samples with varying plastic content (0–50%) and fullerene content (0–0.020%);
- Conduct comprehensive tests of the concrete for compressive strength, impact strength, and freeze–thaw resistance, and examine its microstructure using a scanning electron microscope (SEM);
- Develop mathematical models of the material's properties (RSM) and compare their accuracy with machine learning algorithms (AdaBoost, Random Forest);
- Perform multi-criteria optimisation of the modified concrete mix design using a desirability function.

2. Results

2.1. Research into the Production of Experimental Concrete Specimens for Compressive Test

Table 1 presents data on the compressive strength of concrete mix specimens as a function of plastic and fullerene content. As can be seen from Table 1 and the graphs shown in Figure 1, a decrease in strength is observed in the samples obtained as the ABS plastic content increases. Without the addition of fullerenol, an increase in the plastic content from 0% to 50% leads to a drop in strength at 28 days from 34.81 MPa to 16.33 MPa (a reduction of more than twofold). The total error in strength determination is within ±3.2%.

Table 1. Compressive strength of concrete mix specimens as a function of plastic and fullerene content.

ABS Content in Concrete (Relative to the Mass of Sand), % (by Mass)	Fullerenol Content in the Mixing Water % (by Mass)					
	0.000	0.001	0.003	0.005	0.010	0.020
	Compressive Strength, MPa (7 Days/28 Days)					
0	20.33/34.81	20.80/35.62	21.65/37.08	19.76/33.84	19.27/33.00	18.17/31.12
10	21.30/36.48	20.33/34.82	21.13/36.19	18.65/31.93	15.62/26.74	17.17/29.41
20	19.52/33.43	19.08/32.67	19.52/33.42	18.27/31.28	17.76/30.41	15.29/26.18
30	15.71/26.91	17.33/29.62	16.31/27.93	17.65/30.22	17.54/30.04	16.02/27.43
40	12.28/21.03	15.42/26.41	15.57/26.67	16.87/28.88	16.72/28.64	15.1025.85
50	9.54/16.33	14.32/24.53	15.09/25.84	15.25/26.12	15.75/26.97	14.23/24.36

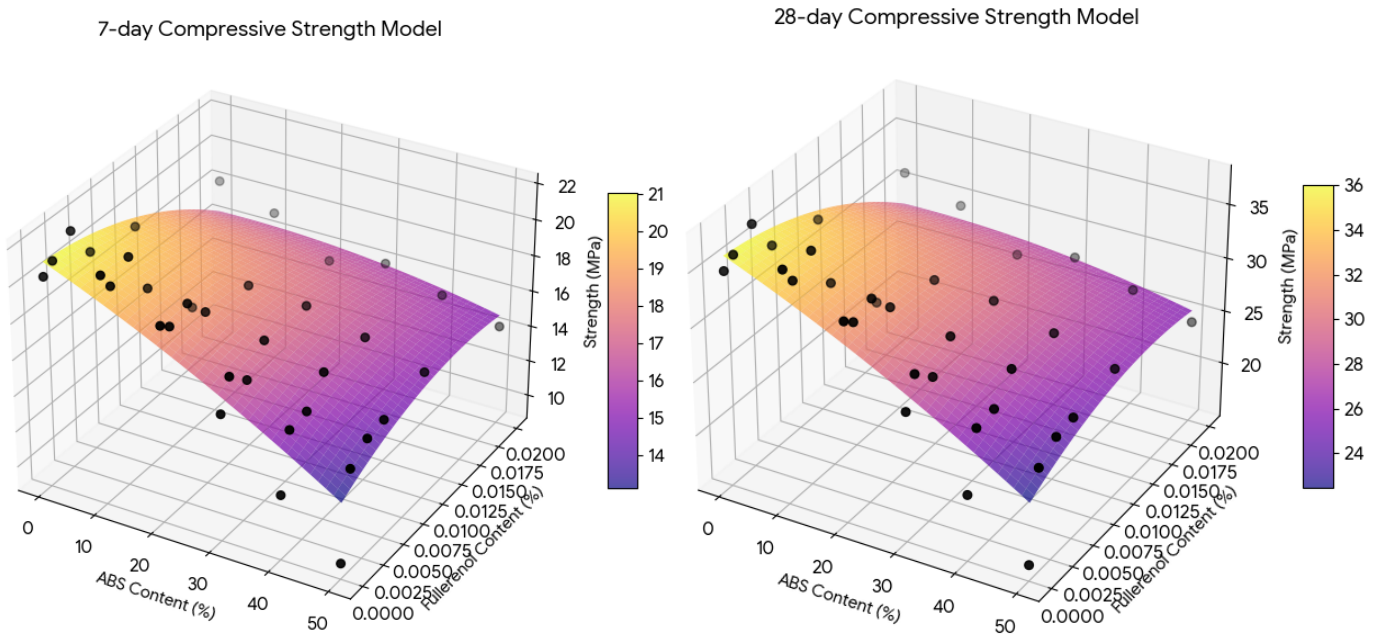


Figure 1. A model of the relationship between the compressive strength of concrete specimens and the concentration of ABS plastic and fullerenol at 7 days (**a**) and 28 days (**b**). The colour scale indicates changes in strength in MPa. The points represent experimental values.

The data obtained are consistent with studies showing a decrease in strength as the proportion of plastic in the concrete mix increases [25]. The addition of fullerenol in low concentrations significantly increases the compressive strength of the mixtures as the plastic content in the concrete composition increases. The best results were recorded at a fullerenol concentration of 0.003–0.010% by mass of water. For mixtures with 50% ABS content, the addition of 0.010% fullerenol increases the strength at 28 days from 16.33 MPa to 26.97 MPa (a 65% increase). At low ABS content (0–10%), the effect of fullerenol is less pronounced or has a weak effect at high dosages (>0.020%). At a fullerenol concentration of 0.020%,

a decrease in strength is observed. To predict the strength of concrete using the data obtained (Table 1), a mathematical model in the form of a quadratic polynomial (regression surface model (RSM)) was developed for the strength of concrete specimens at 7 days of age (1):

$$R_7 = 21.13 - 0.13 \cdot X_1 - 36.19 \cdot X_2 - 0.0008 \cdot X_1^2 + 6.66(X_1 \cdot X_2) - 9949.81 \cdot X_2^2 \quad (1)$$

where X_1—ABS plastic content (% by mass of sand); X_2—fullerene content (% by mass of mixing water). $R^2 = 0.776$. The average error of the model approximation is $\bar{A} = 6.04\%$.

For strength at 28 days (2):

$$R_{28} = 36.19 - 0.22 \cdot X_1 - 61.47 \cdot X_2 - 0.001 \cdot X_1^2 + 11.40 \cdot (X_1 \cdot X_2) - 17049.2 \cdot X_2^2 \quad (2)$$

where X_1 is the ABS plastic content (%), and X_2 is the fullerenol content (%). The model's coefficient of determination was $R^2 = 0.78$ and $\bar{A} = 6.38\%$, which indicates a high degree of fit between the model and the experimental data and is comparable to the model's accuracy for 7-day-old samples. Table 2 shows the values of the regression equation coefficients.

Table 2. The coefficients of the regression equation.

Specifications	b_0 (Const)	b_1 (ABS)	b_2 (Full)
7 days	21.1329	−0.1268	−36.1865
28 days	36.1897	−0.2176	−61.4738

Figure 1 shows RSM plots of strength as a function of: ABS plastic content (X_1) and fullerene content (X_2). The data points represent experimental results, whilst the RSM plots represent mathematical predictions. For 7 days (Figure 1a), strength reaches a maximum in the region of the lowest substitution of sand with plastic (0–5%) and low concentrations of fullerene (up to 0.003%), reaching 21–22 MPa (yellow region). The slope of the surface along the X_1 axis (ABS content (%)) shows a continuous decrease in strength, reaching values >10 MPa at an ABS content of 50%. The introduction of fullerenol at concentrations of 0.005–0.015%, with a plastic content > 40%, 'raises' the surface edge to values of 16–16.5 MPa.

Over a 28-day period (Figure 1b), an increase in strength is observed, reaching a peak of ≈36 MPa. The RSM clearly shows a significant rise in strength in the region where the ABS content is >40%, when fullerene is added in the range of 0.001–0.010%, This allows the formulation with the maximum amount of waste (50% ABS) to achieve strength characteristics of 26–27 MPa, which is comparable to formulations containing 40% less plastic but without a nanomodifier. An increase in the ABS plastic content by more than 10% and in the fullerenol content by more than 0.02% leads to a slight decrease in strength. This can be explained by the aggregation of fullerenol particles, which hinders their uniform distribution and effective participation in the cement hydration process [26,27]. The RSM geometry confirms the adequacy of regression Equations (1) and (2).

2.1.1. A Comparative Analysis of the Accuracy of Predictive Models

Based on the compiled database of experiments (Table 3), a comparative assessment was carried out of the effectiveness of the proposed second-order polynomial model (RSM) and the machine learning algorithms: Random Forest (RF) and AdaBoost. The results of the statistical evaluation of the models on the test sample are presented in Table 3.

Table 3. Statistical measures of accuracy for strength prediction models for 7 and 28 days.

Model	R^2	MAE (Mean Absolute Error), MPa	RMSE (Root Mean Square Error), MPa
Polynomial regression (RSM)	0.776/0.776	0.97/1.66	1.24/2.12
Random Forest (RF)	0.972/0.972	0.33/0.56	0.43/0.74
AdaBoost	0.975/0.977	0.32/0.52	0.41/0.68

An analysis of the data in Table 3 shows that all the models under investigation demonstrate acceptable predictive accuracy ($R^2 > 0.75$). The AdaBoost algorithm yielded the best results, which is consistent with the findings of [24] regarding the high effectiveness of boosting methods in concrete strength prediction tasks. The difference in accuracy between the intelligent algorithms and the classical polynomial model is insignificant (the difference in R^2 is less than 10%). This confirms the adequacy of the RSM analytical equation and the possibility of using it for engineering calculations without the need for complex AI software.

2.1.2. Model Validation and Analysis of Data Dispersion

To provide a visual assessment of the prediction quality, Figure 2 shows the correlation plots between the experimental and predicted strength values for the polynomial model, RF model and the AdaBoost algorithm. The fact that the data points lie close to the line of perfect fit (y = x) indicates the absence of systematic errors. For the RSM, a slightly greater scatter is observed (Figure 2a,d) in the region of low strength values (where the ABS plastic content exceeds 40%), whilst for RF (Figure 2b,e) and AdaBoost (Figure 2c,f), the model adapts more accurately to non-linear changes in the boundary regions. Nevertheless, the RSM clearly illustrates the physical significance of the interaction between the factors (ABS and fullerenol), as expressed through the regression coefficients, which is preferable for understanding the properties of modified concrete.

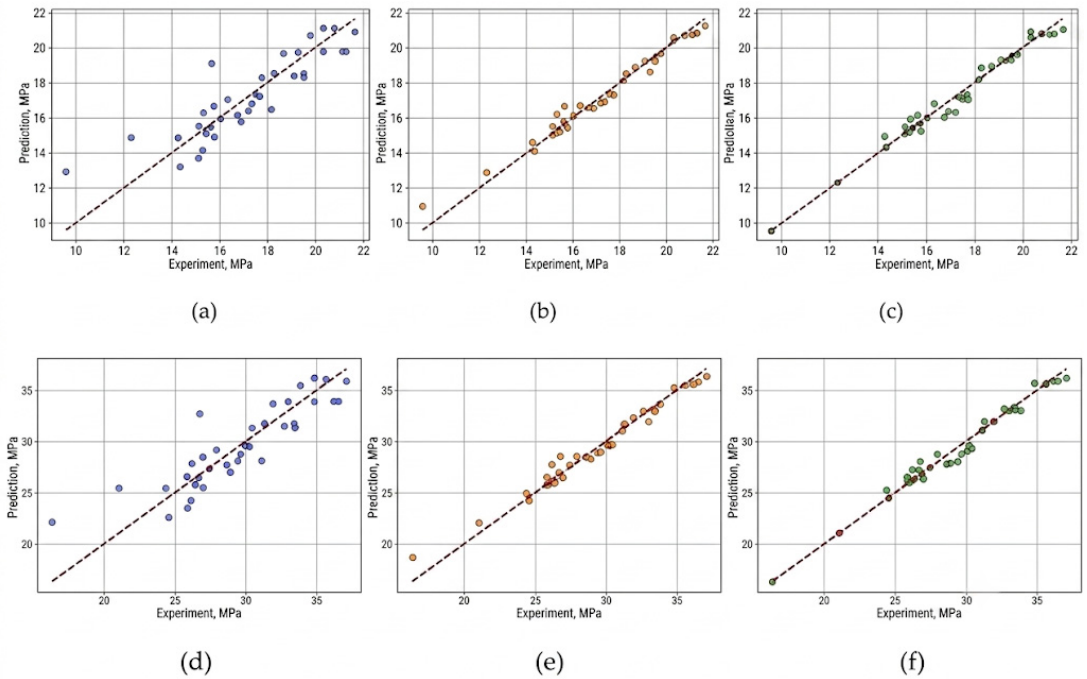


Figure 2. Comparison of experimental and calculated compressive strength values at 7 days: (**a**) RSM; (**b**) RF model; (**c**) AdaBoost model; and at 28 days: (**d**) polynomial model; (**e**) RF model; (**f**) AdaBoost model.

2.2. Research into the Synthesis of Experimental Concrete Specimens for Impact Strength

Table 4 presents data on the impact strength of concrete mix samples as a function of plastic and fullerene content. The total error in the determination of impact strength is within ±5%.

Table 4. The impact strength of concrete mix samples as a function of plastic and fullerene content.

ABS Content in Concrete (Relative to the Mass of Sand), % (by Mass)	Fullerenol Content in the Mixing Water % (by Mass)					
	0.000	0.001	0.003	0.005	0.010	0.020
	Energy at Initial Cracking, J_i (J)/Energy at Final Failure, J_f (J)/Ductility Index (J_i/J_f)					
0	156.61/285.85/1.822	158.05/285.89/1.8	298.25/160.13/1.86	289.98/159.16/1.82	285.85/158.71/1.8	273.45/158.65/1.72
10	148.17/281.14/1.89	151.5/281.00/1.85	293.4/160.23/1.83	281.00/154.37/1.82	289.27/157.74/1.83	276.87/157.8/1.75
20	142.34/269.76/1.895	141.28/273.96/1.93	278.02/150.13/1.85	269.76/146.02/1.84	265.63/145.88/1.82	265.63/143.76/1.84
30	126.54/256.21/2.02	127.14/252.08/1.98	260.34/134.74/1.93	252.08/126.5/1.99	243.81/127.26/1.91	227.28/128.05/1.77
40	106.24/235.55/2.21	110.44/235.55/2.13	247.94/113.72/2.18	243.81/105.4/2.31	235.55/109.53/2.15	219.02/105.61/2.07
50	93.78/223.15/2.37	98.02/219.02/2.23	227.28/97.80/2.43	223.15/92.31/2.41	219.02/97.56/2.24	206.62/98.10/2.1

To predict the impact strength of concrete using the data obtained (Table 4), a mathematical model was developed (in the form of a quadratic polynomial (regression surface model (RSM)). Table 5 shows the coefficients of the regression equation.

Table 5. The coefficients of the regression equation.

Specifications	b_0 (Const)	b_1 (ABS)	b_2 (Full)
7 days	290.117	−0.778	766.756

The second-order regression Equation (3) for impact toughness (J_f):

$$J_f = 290.117 - 0.778 \cdot X_1 + 763.756 \cdot X_2 - 0.0116 \cdot X_1^2 - 9.96 \cdot (X_1 \cdot X_2) - 64832.225 \cdot X_2^2 \quad (3)$$

where

X_1—ABS content (%);

X_2—Fullerenol content (%).

The coefficient of determination of the model is $R^2 = 0.954$. The average error of the model approximation is $\bar{A} = 2.05\%$.

Figure 3 shows the RSM of the impact strength of concrete specimens as a function of the concentration of ABS plastic and fullerenol. The black points on the graph represent the actual experimental values. The fact that the points lie in close proximity to the RSM confirms the high accuracy of Equation (3). The points in the region of low fullerenol additions lie above the level of concrete without additives, which is mathematically confirmed by the positive coefficient of +763.756 for the linear term X_2. With an increase in plastic content (X_1) from 0 to 50%, a steady decrease in impact strength is observed, which is reflected in the graph by the downward slope of the curve along the ABS content axis. Fullerenol (X_2) exhibits the properties of a viscosity modifier. Its effect is extreme in nature: at low concentrations (up to 0.005%), the curve shows a local rise, and with a further increase in dosage, a decline begins, caused by the overdosing effect.

The 'Yellow Zone', with maximum values of 280–295 (J), is located in the corner with the lowest ABS content (0–10%) and the optimal fullerene dosage (0.001–0.005%). The 'green-blue zone', with values of 240–270 (J), represents mixtures where the negative effect of plastic is partially offset by the strengthening effect of fullerene. The 'purple zone', with minimum values of 200–220 (J), corresponds to mixtures with the maximum ABS content (40–50%) and an excess of fullerene (0.020%). In this region, the impact strength decreases by almost 30% from the initial value.

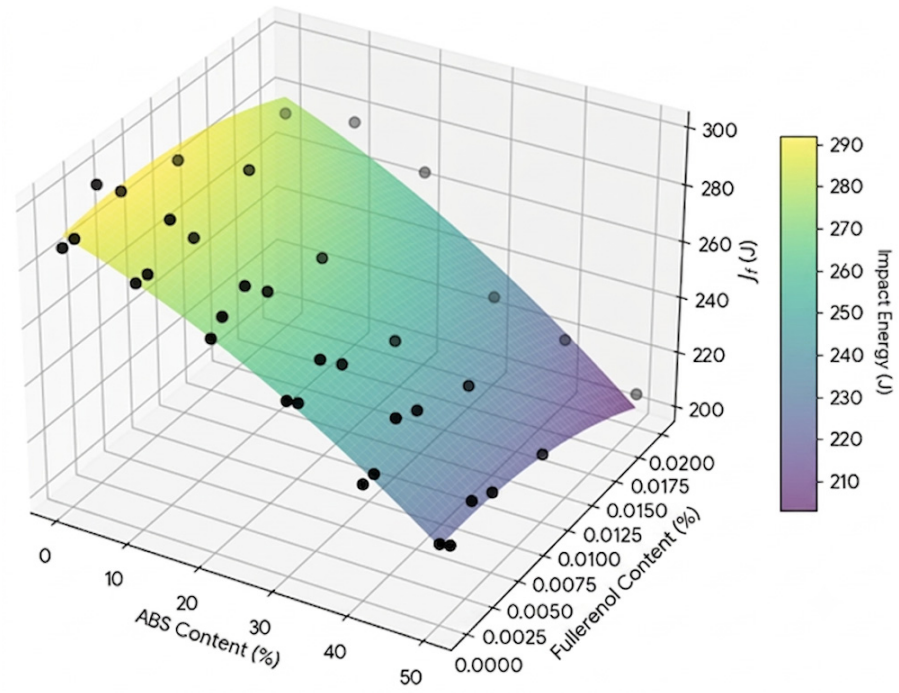


Figure 3. A model of the relationship between the impact strength of concrete specimens and the concentration of ABS plastic and fullerene (RSM). The colour scale reflects the change in the specimen's total impact strength in joules. The points represent the experimental values.

2.2.1. A Comparative Analysis of the Accuracy of Predictive Models

Based on the compiled database of experiments (Table 4), a comparative assessment was carried out of the effectiveness of the proposed second-order polynomial model (RSM) and the machine learning algorithms: Random Forest (RF) and AdaBoost. The results of the statistical evaluation of the models on the test sample are presented in Table 6. According to the results of the statistical analysis, all models demonstrated high prediction accuracy ($R^2 > 0.95$).

Table 6. Statistical indicators of the accuracy of models for predicting the impact strength of concrete specimens.

Model	R^2 (Coefficient of Determination)	MAE (Mean Absolute Error), J
RSM (Polynomial)	0.954	4.51
Random Forest (RF)	0.993	1.76
AdaBoost	0.990	1.98

2.2.2. Model Validation and Analysis of Data Dispersion

Figure 4 shows plots comparing experimental impact toughness values (J_f) with data obtained using three different prediction methods: polynomial regression (RSM), random forest (RF) and the AdaBoost algorithm. For all three models, there is a high concentration of data points along the line of best fit across the entire range of values (from 200 to 300 J), which confirms the correctness of the selected training parameters. RSM demonstrates a coefficient of determination $R^2 = 0.954$ (Figure 4a). The graph shows slight deviations of the data points from the central line, indicating that the quadratic equation, whilst describing the general trend, may overlook some complex non-linear interactions between components. RF showed the best result with $R^2 = 0.993$ (Figure 4b). The data points on the graph practically merge with the line of perfect fit, indicating a minimal mean absolute error (MAE = 1.76 J) and the model's ability to capture patterns with extreme accuracy, even at the extreme values of the sample.

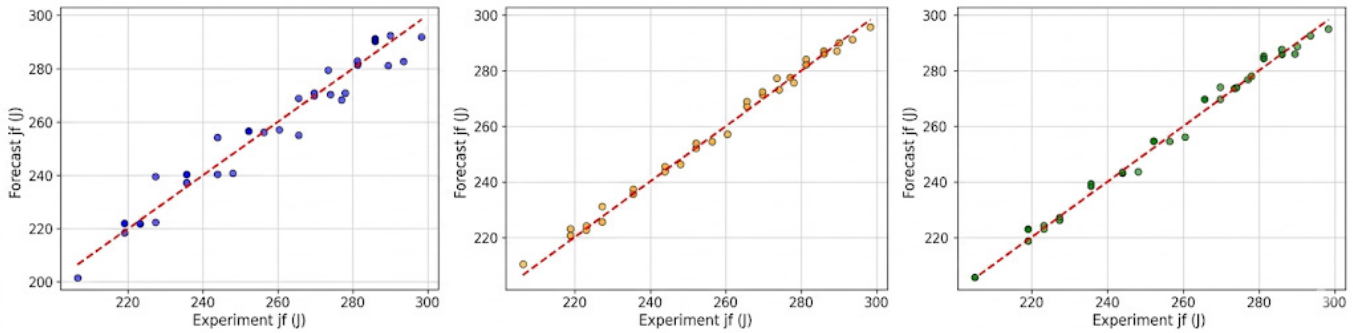


Figure 4. Comparison of experimental and calculated values of the impact strength of concrete specimens: (**a**) polynomial model; (**b**) RF model; (**c**) AdaBoost model.

AdaBoost (Figure 4c) also demonstrated high accuracy (R^2 = 0.99). The graph is identical to that of the RF model, showing only a slight increase in dispersion in the range of average values (240–260 J). It can be seen that the machine learning models (RF and AdaBoost) outperform the classical analytical RSM in terms of the accuracy of the approximation of the experimental data. However, the high concentration of points on the RSM graph (R^2 > 0.95) confirms the adequacy of the derived regression Equation (6) and the possibility of using it for engineering calculations of the impact strength of concrete with ABS and fullerenol additives.

2.3. Frost Resistance

Table 7 presents the results of concrete freeze–thaw resistance tests. The highest number of cycles (N = 143) was recorded in the control sample containing 0.003% fullerene, yet it was in this series that the sharpest decline in freeze–thaw resistance was observed when 30% plastic was added (down to N = 53). Formulations 0.01 and 0.02 demonstrate the most 'stable' results. The maximum permissible range of variation in results within a series does not exceed 5.9%.

Table 7. Results of concrete frost resistance tests.

Composition of the Sample (Additive, %)	Fullerene (%)	Frost Resistance Rating (F)	Actual Number of Cycles (N)
0%	0	F100	116
10%	0	F75	94
20%	0	F100	113
30%	0	F75	84.5
0%	0.001	F100	109
10%	0.001	F75	89
20%	0.001	F75	89
30%	0.001	F75	85
0%	0.003	F100	143
10%	0.003	F75	81
20%	0.003	F75	81
30%	0.003	F50	53
0%	0.005	F75	94
10%	0.005	F75	94
20%	0.005	F75	91
30%	0.005	F75	88
0%	0.01	F100	103
10%	0.01	F100	107
20%	0.01	F75	92
30%	0.01	F75	99
0%	0.02	F100	104
10%	0.02	F75	98
20%	0.02	F75	95
30%	0.02	F75	81

Even with a 30% plastic additive, the actual number of cycles remains within the range of 81–99, which is significantly higher than that of the 0.003 series. In all series except 0.01, a decrease in frost resistance is observed as the plastic additive content increases. Most samples with 10–30% additives move from category F100 to F75. According to the data obtained, mathematical model (4) takes the following form:

$$N = 113.13 - 1.52 \cdot X_1 - 588.03 \cdot X_2 + 0.015 \cdot {X_1}^2 + 8471.34 \cdot {X_2}^2 + 28.30 \cdot (X_1 \cdot X_2) \quad (4)$$

where:

X_1—ABS content (%);

X_2—Fullerenol content (%).

The coefficient of determination of the model is R^2 = 0.84. The average error of the model approximation is $\bar{A}$ = 7,14%.

Figure 5 presents a model of the relationship between the actual number of cycles (N) and the plastic content (P) and fullerene dosage (F) in the form of an RSM.

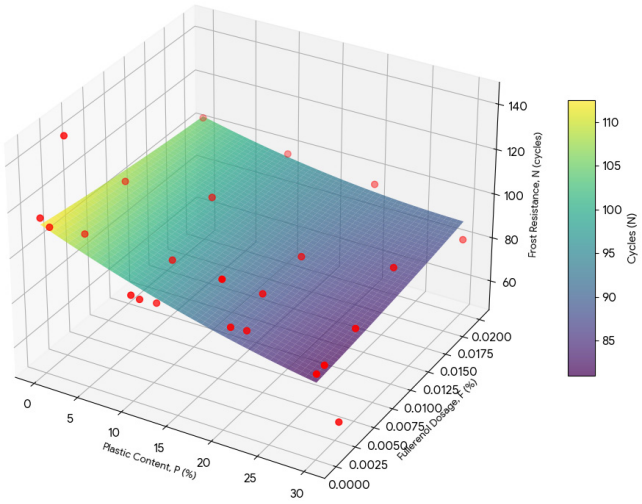


Figure 5. A model showing the relationship between the frost resistance of concrete specimens and the concentration of ABS plastic and fullerene (RSM). The colour scale indicates changes in frost resistance. The points represent experimental values.

The linear coefficient (−1.52) confirms that plastic is the main factor reducing frost resistance (4). The interaction of factors (coefficient +28.30 for $X_1 \cdot X_2$) indicates that at high plastic concentrations, fullerene begins to exert a more pronounced stabilising effect on the concrete structure. The RSM in the yellow and light green areas shows parameters where frost resistance remains above 100 cycles. This is typical for mixtures with a plastic content of up to 15% and a fullerene dosage of around 0.01%.

A Comparative Analysis of the Accuracy of Predictive Models

Table 8 presents a comparative analysis of classical regression against machine learning algorithms, specifically Random Forest (RF), AdaBoost and RSMs.

Table 8. Statistical indicators of the accuracy of models for predicting the frost resistance of concrete specimens.

Model	R^2 (Coefficient of Determination)	MAE (Mean Error), J
RSM (Polynomial)	0.84	8.4
Random Forest (RF)	0.91	5.2
AdaBoost	0.88	6.7

RSM demonstrates high sensitivity to plastic (coefficient −1.52 X_1). It is effective for determining the 'safety zone' (the yellow area in Figure 6); however, the calculated minimum at X_1 = 30% and X_2 = 0.003% is higher than the actual value (53 cycles), which indicates the presence of hidden structural defects that the quadratic model does not capture. Figure 6 shows a graph comparing the experimental and calculated values of the frost resistance of concrete specimens using RSM (Figure 6a), RF (Figure 6b) and AdaBoost (Figure 6c). AdaBoost shows smallest scatter in the middle range (80–110 cycles). RSM has the greatest scatter, deviating noticeably from the line in the lower and upper parts of the graph. RF shows the most balanced accuracy.

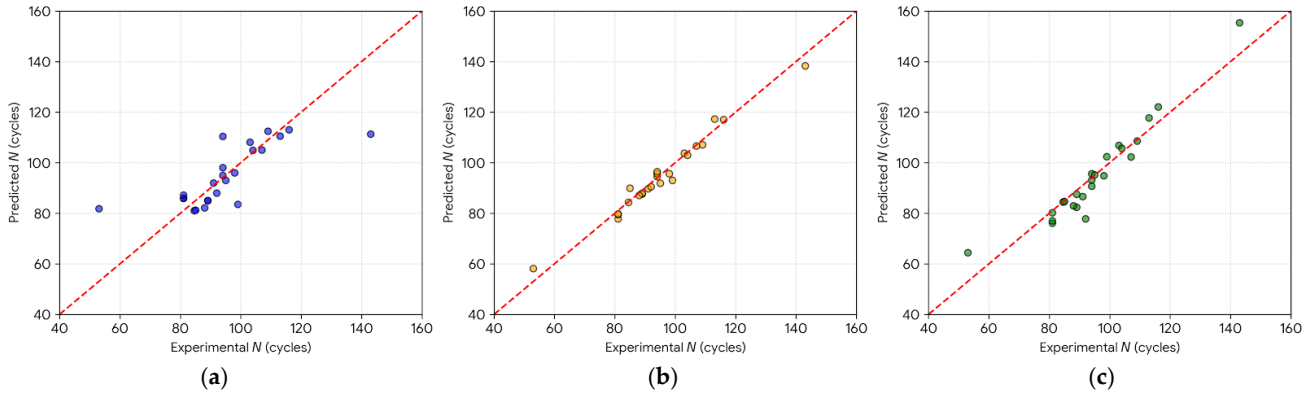


Figure 6. Comparison of experimental and calculated values for the frost resistance of concrete specimens: (**a**) RSM; (**b**) RF model; (**c**) AdaBoost model.

2.4. Optimisation of the Concrete Mix Design Based on the Data Obtained

Figure 7 shows a general graph (contour map) of multi-criteria optimisation. The general equation for the desirability function 5 (in the desirability interval 0–1) is as follows:

$$D = 0.82 - 0.009 \cdot X_1 + 12.45 \cdot X_2 - 0.0001 \cdot X_1^2 + 0.15(X_1 \cdot X_2) - 850.5 \cdot X_2^2 \quad (5)$$

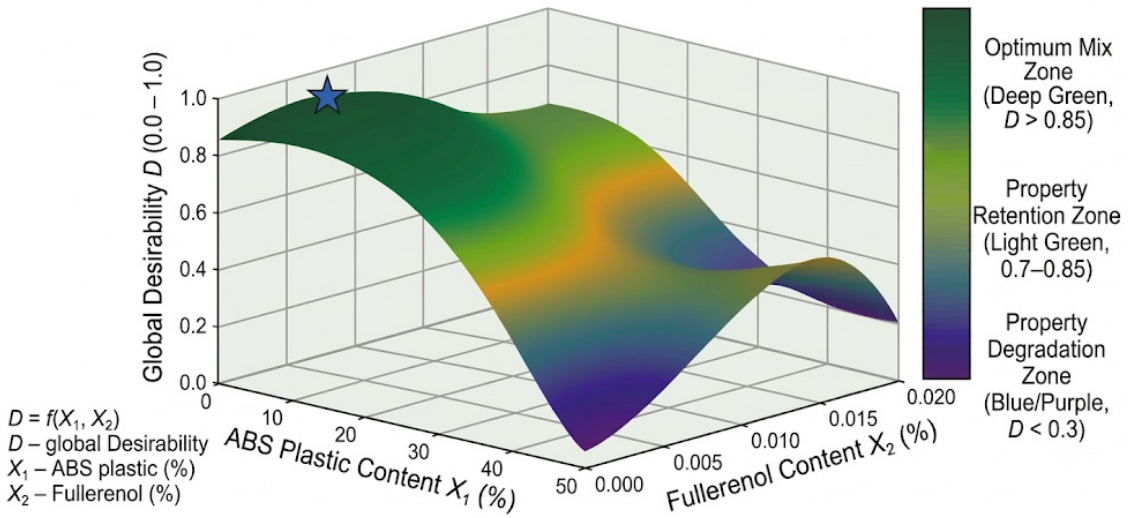


Figure 7. A model showing how the properties of concrete samples vary with the concentration of ABS plastic and fullerene. The colour scale illustrates the changes in the properties of the concrete samples.

The coefficient of determination of the model is R^2 = 0.854, The average error of the model approximation is $\bar{A}$ = 5.21%.

It combines data on compressive strength, impact strength and frost resistance. The dark green zone corresponds to formulations offering the best combination of all three char-

acteristics. The optimal point (blue star) is at a plastic concentration of 0%. The range up to 5–7% plastic content (light green zone) and a fullerene content of 0.006–0.008% ensures that high performance properties are maintained. In this range, fullerene most effectively compensates for the reduction in strength and toughness by creating a dense microstructure.

The highest point on the surface (the dark green area) is located at coordinates X_1 0–5% and X_2 0.007%. Here, the D value exceeds 0.85, which corresponds to the 'very good' category on the Harrington scale. When up to 10% plastic is added, the surface does not drop vertically but follows a gentle slope. This is visual proof that fullerene 'holds' the concrete structure together, offsetting the negative impact of the polymer. After the 30% mark on the X_1 axis, the surface drops sharply into the 'blue' zone ($D < 0.3$). This is the region where neither the physical properties nor the durability meet the requirements, regardless of the fullerenol dosage. At $X_2 > 0.015\%$, the edge of the surface begins to curve downwards smoothly. This reflects the effect of reduced strength due to the aggregation of nanoparticles at high concentrations.

3. Discussion

3.1. The Effect of Fullerene on the Strength of Concrete

Analysis of the experimental data and the resulting response surfaces reveals the dual role of fullerenol in determining the strength characteristics of modified concrete. Fullerenol acts as an effective nanomodifier capable of partially compensating for the reduction in strength caused by the addition of plastic waste. When the ABS plastic content ranges from 30% to 50%, a marked increase in strength is observed upon the introduction of small doses of fullerenol (0.001–0.010% by weight of water). For example, for samples with a 50% ABS content, the strength on the 28th day increases from 16.33 MPa (without fullerenol) to 26.97 MPa at a fullerenol concentration of 0.010%. This corresponds to a strength increase of ≈65% relative to a composition with a similar plastic content but without added fullerenol. The increase in strength upon the addition of fullerenol is explained by its ability to act as an active nanoscale centre that initiates processes of structural densification of the matrix.

Fullerenol molecules tend to form stable hydrates and significantly affect the solubility of the mixture's components [28]. This may contribute to the accelerated formation of cement paste microcrystals directly in the transition zone of contact with hydrophobic ABS plastic, compensating for its low adhesion and densifying the C-S-H gel structure. The plastic filler (ABS) has weak adhesion to the cement matrix and creates additional voids. Fullerene, due to its high specific surface area, helps reduce the influence of microdefects and strengthen the transition zone. Figure 8 shows the topology of concrete samples with 0% plastic content, with 0.003 fullerenol added (Figure 8a,c) and without 0.003 fullerenol added (Figure 8b,d). Figure 8a (×50) and Figure 8c (×200) show a more homogeneous and dense cement matrix structure with a minimal number of micro cracks. The diameter of the spherical air pores in Figure 8a does not exceed 20 μm. Figure 8b (×50) shows large spherical air pores with diameters ranging from 200 to 600 μm. The cement stone matrix appears fairly dense, with a uniform distribution of aggregate grains. Figure 8d (×200) shows a surface with more pronounced inhomogeneities. It can be visually observed how the addition of fullerenol (Figure 8a,c) contributes to a reduction in the number of microdefects at phase boundaries, which correlates with an increase in the strength characteristics of the concrete.

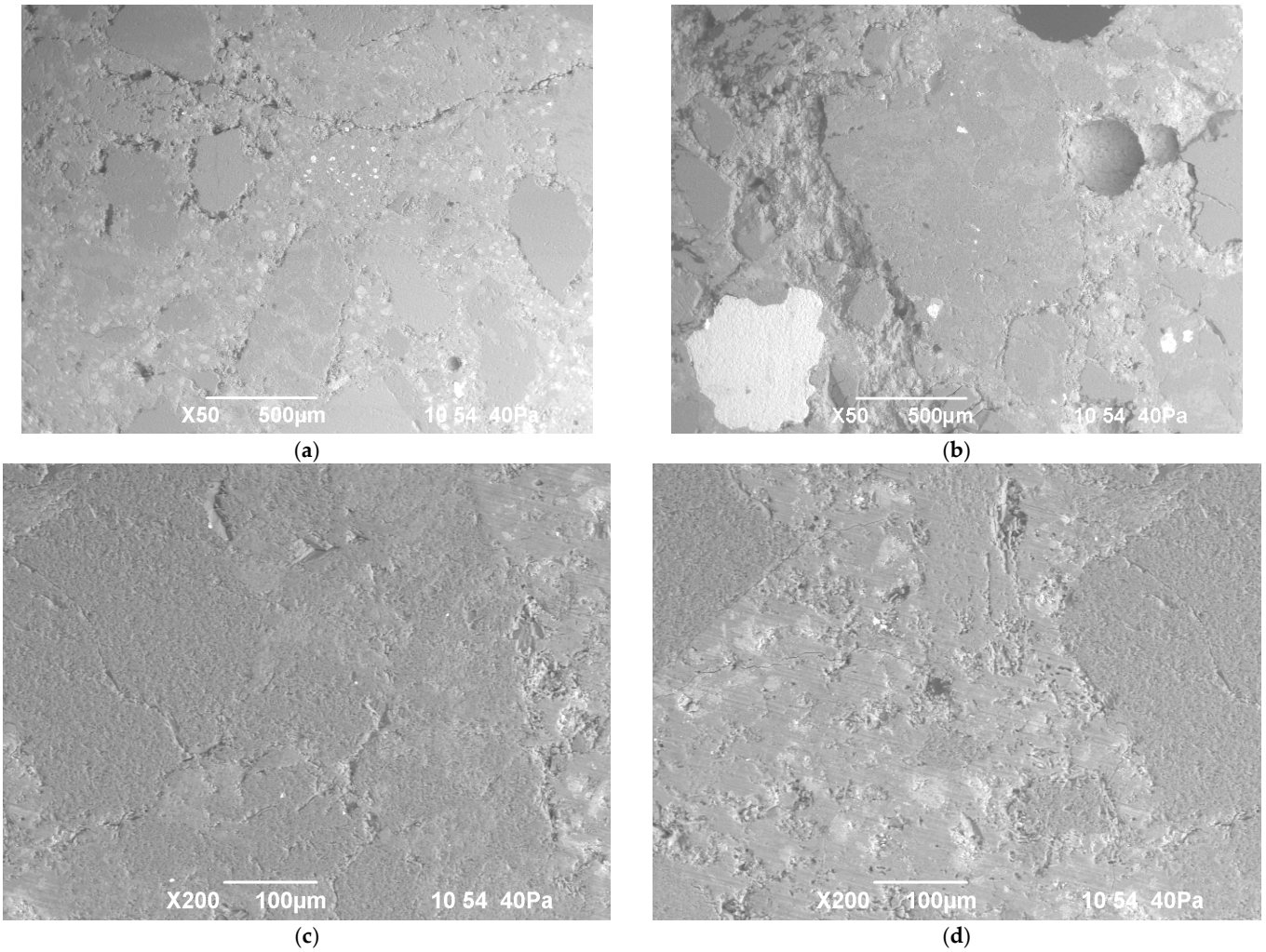


Figure 8. Microphotographs of a concrete sample with 0% plastic content, with 0.003% fullerenol added (**a**,**c**) and without 0.003% fullerenol added (**b**,**d**).

Figure 9 shows the microstructure of concrete specimens containing 30% plastic, with 0.003% fullerene added (Figure 9a,c) and without 0.003% fullerene added (Figure 9b,d). Figure 9a (×50) shows a relatively uniform distribution of aggregate and plastic inclusions. The matrix appears cohesive, with fewer macropores. Figure 9c (×200) shows that the contact zone between the particles and the cement paste is denser. Fullerenol minimises the negative impact of the polymer additive on the overall structural integrity. In Figure 9b (×50), large interphase voids and irregularly shaped cavities are clearly visible. In Figure 9d (×200), delamination of the cement paste from the aggregate surface is observed. The mathematical models (Equations (1) and (2)) confirm the non-linear effect of the nano-additive. The negative coefficient of the quadratic term X_2^2 (−17,049.2 for 28 days) indicates the presence of an optimal concentration; exceeding this concentration leads to a decrease in effectiveness. At fullerenol concentrations above 0.020%, a plateau or decrease in strength is observed. This may be related to the agglomeration of nanoparticles, where, instead of being distributed within the pores, excess particles form clusters that themselves become stress concentrators within the concrete structure. The positive coefficient for the X_1X_2 interaction (+11.40 for 28 days) mathematically demonstrates that the positive effect of fullerenol increases as the ABS plastic content rises (2). While RSM polynomial equations provide a transparent interpretation of the components' influence on concrete strength, the use of machine learning algorithms (RF and AdaBoost) allows for a significant reduction in prediction uncertainty. Unlike the RSM, which smooths dependencies down to

quadratic forms, intelligent methods more effectively capture local nonlinearities arising in critical zones (for example, at extremely high ABS plastic content or at the onset of intense nanoparticle aggregation).

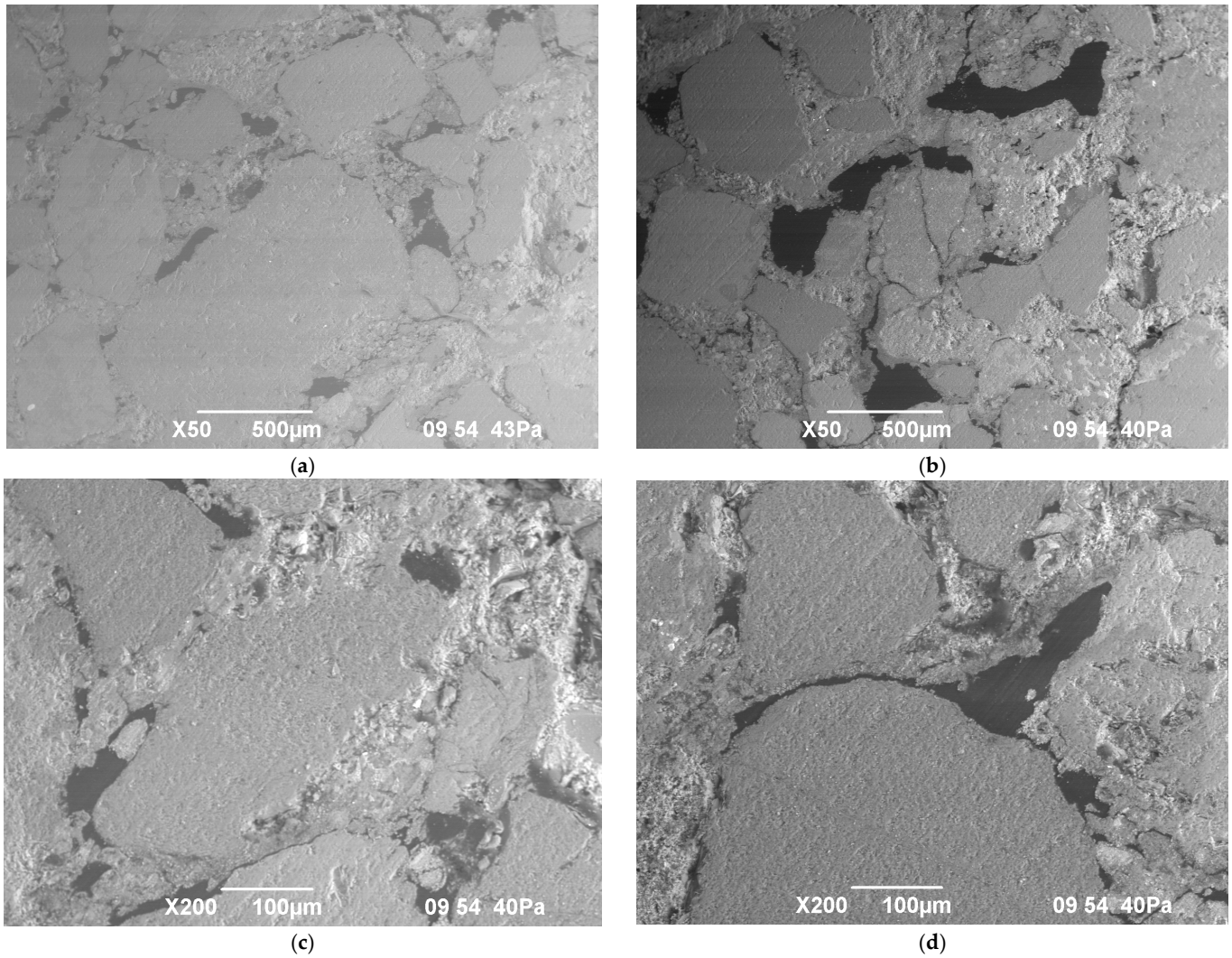


Figure 9. Microphotographs of a concrete specimen containing 30% plastic, with 0.003 g of fullerenol added (**a**,**c**) and without 0.003 g of fullerenol added (**b**,**d**).

The high values of the coefficient of determination ($R^2 > 0.99$) for the AdaBoost and Random Forest models indicate that these algorithms are capable of compensating for the "noise" caused by the non-uniform distribution of recycled plastic in the concrete matrix. Thus, the application of AI methods serves as a powerful verification tool: it confirms that the residual error of the RSM analytical model is due not to random data variation, but to the simplification of the mathematical description of a complex multiphase system, which, however, remains acceptable for practical engineering calculations.

3.2. The Effect of Fullerene on the Impact Strength of Concrete

An increase in the ABS plastic content leads to a gradual decrease in impact strength (Jf). Analysis of the coefficients in Equation (3) shows that the fullerene content makes the greatest contribution to the increase in impact strength (X_2 = +763.756). The high positive value of this linear coefficient confirms the role of the nanomodifier as a key agent in increasing the energy absorption at fracture. The significant negative coefficient for the square of the fullerenol concentration (X_2^2 = −64,832.225) accounts for the parabolic nature

of the curve. This indicates the attainment of a 'saturation limit', beyond which the further introduction of nanoparticles causes their agglomeration and a decrease in toughness. The negative value of the pair interaction coefficient ($X_{12} = -9.960$) indicates the need for a strict balance between ABS plastic and fullerenol: an excess of both simultaneously creates an effect of structural supersaturation, which reduces impact strength. The response surface takes the form of a pronounced dome (extreme). The maximum impact strength values (the dark red area) are achieved at ABS plastic concentrations in the range of 2.5–7.5% and fullerene concentrations of 0.005–0.007%. In this region, the calculated Jf values peak at 310–315 J, which significantly exceeds the values for the control compositions. The high agreement between the theoretical surface and the experimental results (marked by black dots) confirms the adequacy of the model. The location of the dots near the apex of the dome demonstrates that the selected ranges of factor variation have successfully identified the region of optimal physical and mechanical properties of the composite. Thus, the combined modification with ABS plastic and fullerene provides a synergistic effect, contributing to the formation of a more viscous concrete matrix capable of effectively absorbing impact energy by inhibiting microcracks at the nano- and micro-levels.

3.3. The Effect of Fullerene on the Frost Resistance of Concrete

Analysis using all methods confirms that the addition of fullerene in the range of 0.01–0.02% counteracts the negative effects of recycled ABS plastic. Instability is observed at low fullerene dosages (0.001–0.003%). It is likely that a small amount of the nanomodifier is insufficient to create a continuous reinforcing layer, which, when 30% plastic is added, leads to a critical increase in porosity and a drop in N to 53. At optimal dosages (0.01%), the RF and AdaBoost models show stabilisation of the N value at 90–100 cycles even with high plastic content. This is explained by the formation of a denser microstructure capable of withstanding the pressure of ice in the pores. Thus, the use of ensemble machine learning methods (RF and AdaBoost) confirmed the high predictive ability of the mathematical model (4), whilst revealing that for compositions with high heterogeneity (30% plastic), the use of Random Forest provides a more accurate prediction of durability than the classical.

3.4. Determining the Optimal Formulation Based on the Tests Carried out

When the plastic content exceeds 10%, the quality index drops sharply (moving into the blue and yellow zones). This is because plastic reduces adhesion and durability. Fulleronol acts as a stabiliser. When plastic is added, a correctly selected dose of fullerenol allows the limits of high-quality concrete to be 'shifted' towards higher additive concentrations. The most rational composition from an environmental (plastic recycling) and technical perspective is the use of 5% plastic and 0.007% fullerenol.

4. Materials and Methods

The concrete mixtures were prepared using crushed stone, quartz sand, recycled ABS plastic from electronic waste, mixing water with nano-additives, Portland cement, and a plasticizer (Master Rheobuild 1000, density of 1.204 g/cm^3). All concrete mixtures were prepared with a constant water-to-cement ratio (w/c) of 0.63. Crushed stone and quartz sand (bulk density 1787 kg/m^3) produced by «Kombinat Nereudnykh Materialov» LLP, Ust-Kamenogorsk, East Kazakhstan, were manufactured in accordance with ASTM C33/C33M [29]. Portland cement M500 (manufactured by «Bukhtarma Cement Company» LLP, Oktyabrsky settlement, Kazakhstan) was used as the binder. The chemical composition and some physical and mechanical parameters of Cement M500 as provided by the manufacturer are shown in Table 9. The composition of the mixing water can significantly affect the quality of the concrete (setting time and strength development). The review [30]

thoroughly examined the beneficial and harmful effects of each alternative source of drinking water. Therefore, tap water supplied by the state-owned utility «Oskemen Vodokanal» (Ust-Kamenogorsk, Kazakhstan) was used as the mixing water.

Table 9. Average chemical and phase composition of the cement with brand M500 (Bukhtarma Cement Company, Kazakhstan).

Name of Product	Content Of Oxides (Mass. %)								Compressive Strength, MPa	Density, kg/m^3
	SiO_2	Al_2O_3	Fe_2O_3	CaO	MgO	SO_3	$Na_2O + K_2O$	Others		
Cement M500	22.40	3.27	2.40	67.51	1.26	0.52	1.86	0.78	48	1300

The water meets the requirements of EN 1008:2002 [31]. ABS plastic (acrylonitrile butadiene styrene) was used as a partial substitute for the fine aggregate–quartz sand. The ABS plastic was obtained in a university laboratory by dismantling end-of-life personal computer monitors. The monitor casings underwent a two-stage crushing and screening process using a −5 + 2.5 mm sieve to eliminate the influence of particle size on the properties of the slurry and concrete, since particle size and size distribution affect the interfacial transition zone between the aggregate particles and the cement paste [32]. The plastic was then rinsed in tap water and dried. The topography and microstructure of the sample surfaces were examined using a JSM-6390LV scanning electron microscope manufactured by JEOL Ltd. (Akishima, Tokyo, Japan). A diagram of the preparation of the synthetic filler–ABC plastic is shown in Figure 10. As a result, a ground synthetic filler was obtained.

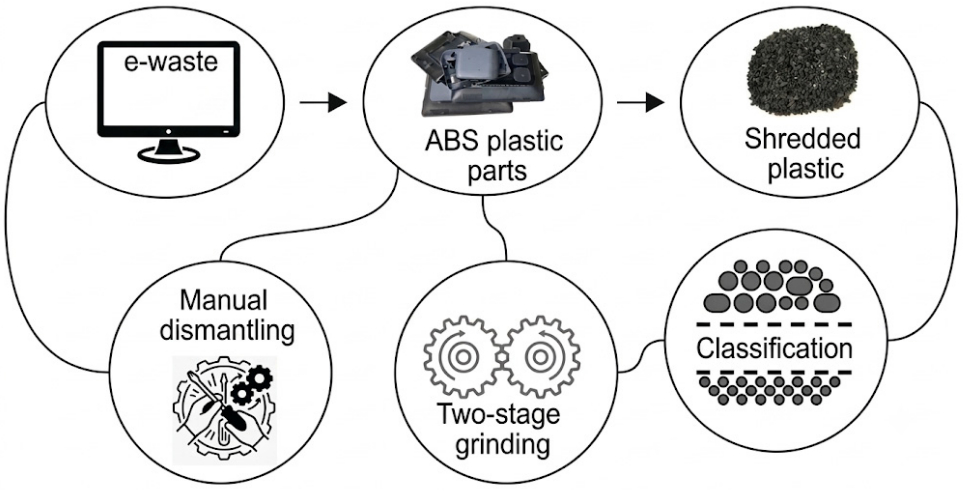


Figure 10. Process for producing a synthetic filler–ABS plastic.

4.1. Synthesis of Experimental Concrete Specimens

Crushed stone, sand and plastic were weighed, loaded into the mixer and mixed for 2–3 min. ABC shredded plastic was added to the concrete mix at levels of 0, 10, 20, 30, 40 and 50 per cent of the mass of the fine natural aggregate–sand. M500 cement was then added to the resulting aggregate mixture and mixed for 2–3 min. The required amount of plasticiser was dissolved in the mixing water. The resulting solution was added to the mixer containing the aggregate and cement mixture and mixed for 10 min. The resulting concrete mixture was poured into moulds and placed on a vibrating table for compaction. All mixtures were compacted until the release of air bubbles ceased. The experimental concrete specimens were covered with a tight-fitting film and removed from the moulds after 24 h. The experimental concrete specimens were then placed in a curing chamber under

standard conditions: temperature 20 ± 2 °C, relative humidity 95 ± 5%, in accordance with EN 12390-2:2009 [33].

The nanomaterial—fullerenol-m—was added to the concrete mix together with the mixing water, at ratios of 0.001%, 0.003%, 0.005%, 0.01% and 0.02% by mass.

For each concrete mix composition, four samples were tested, and the average value of the parameter under investigation was subsequently taken into account.

The study examined the effect of curing time (7 and 28 days) on compressive strength, and 28 days on impact strength and frost resistance. During the research, 288 experimental concrete specimens were produced for the compressive strength test: 48 specimens containing only ABC plasticiser and 240 specimens (144 each for 7 and 28 days) with the addition of ABC plastic and fullerene-M (cubes with an edge length of 150 mm). For the impact test, 144 experimental concrete specimens were produced: 24 specimens containing only ABC plastic and 120 specimens containing ABC plastic and fullerenol-m (cylinders with a diameter of 152 mm and a height of 63.5 mm). A flowchart illustrating the stages of synthesis of the experimental concrete specimens is shown in Figure 11.

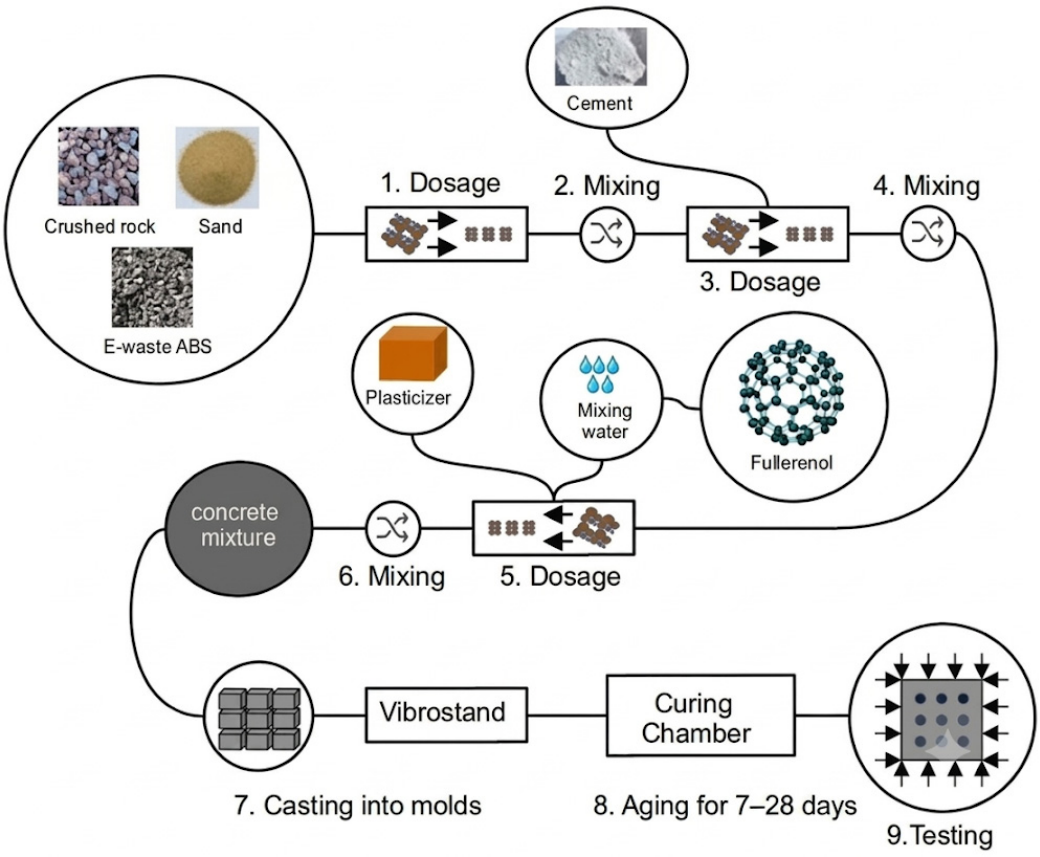


Figure 11. Flowchart for the production of experimental concrete samples.

The composition of the concrete mix used in the production of the experimental specimens (expressed in kg per 1 m^3 of concrete mix) is shown in Table 10. All ingredients of the concrete mix were weighed on electronic scales to an accuracy of 0.01 g.

Table 10. Composition of the concrete mix used in the production of experimental specimens (expressed in kg per 1 m^3 of concrete mix).

ABC Plastic Content, % (by Mass of Sand)	0	10	20	30	40	50
Portland cement (M 500)						
Usage per 1 cube, g	1139	1139	1139	1139	1139	1139
Consumption per 1 m^3, kg	285	285	285	285	285	285
Crushed stone						
Usage per 4 cubes, g	4177	4177	4177	4177	4177	4177
Consumption per 1 m^3, kg	1044	1044	1044	1044	1044	1044
Sand						
Usage per 4 cubes, g	4856	4370	3884	3399	2914	2428
Consumption per 1 m^3, kg	1214	1092	971	850	728	607
Plastic						
Usage per 4 cubes, g	0	140	279	419	560	700
Consumption per 1 m^3, kg	0	35	70	105	140	175
Curing solution						
Usage per 4 cubes, g	715.5	715.5	715.5	715.5	715.5	715.5
Consumption per 1 m^3, kg	179	179	179	179	179	179
Plasticiser						
Usage per 4 cubes, g	17.08	17.08	17.08	17.08	17.08	17.08
Consumption per 1 m^3, kg	4.27	4.27	4.27	4.27	4.27	4.27

4.2. Addition of Nanomaterial

A water-soluble modification of fullerene, fullerenol-m, was used as the nanomaterial. The synthesis and identification of this fullerenol-m sample were studied in [34]. Fullerenol-m used in the experiments contained 98–99% by weight of the main substance. The nanopreparation was added to the concrete mixture with mixing water. Table 11 presents data on the amount of fullerene in the concrete mixture samples.

Table 11. Data on the amount of fullerene in concrete mix samples.

Content in the Concrete Mix (by Mass, %)	Consumption of F per 1 Cube, g	F Consumption for 4 Cubes, g	Consumption of F per 1 m^3 of Concrete, g
0	0	0	0
0.001	0.007	0.029	7.154
0.003	0.021	0.087	21.462
0.005	0.036	0.143	35.769
0.01	0.072	0.286	71.538
0.02	0.143	0.572	143.077

4.3. Testing and Research Methods

4.3.1. Compressive Strength

Concrete specimens containing varying amounts of plastic were removed from the curing chamber. Once the residual moisture had evaporated from the surface of the specimens, they were placed in a PGM-100MG4 hydraulic press (Zapadpribor, Lviv, Ukraine). Measurements were carried out in accordance with EN 12390-3:2019 [35]. The loads applied to the specimens until failure were determined as the ultimate loads. The average compressive strength of the concrete was assessed at curing ages of 7 and 28 days.

4.3.2. Determination of the Impact Strength of Samples

The impact strength was determined in accordance with ACI 544-2R [36]. The method is simple and effective [37,38]. The number of impacts required to produce the first visible crack and the total number of impacts causing the specimen to fail are determined.

A 4.45 kg mass is dropped from a height of 457 mm onto a steel ball positioned above the specimen. The test rig ensures that the ball and specimens are securely fixed. A general view of the test rig is shown in Figure 12. The impact energy was determined using Equation (6), where

$$W = n \cdot m \cdot g \cdot h \quad (6)$$

where h is the drop height of the impact weight, m is the mass of the impact weight, n is the number of impacts applied, and g is the acceleration due to gravity (9.81 m/s^2). The impact strength of the concrete was assessed after 28 days of curing.

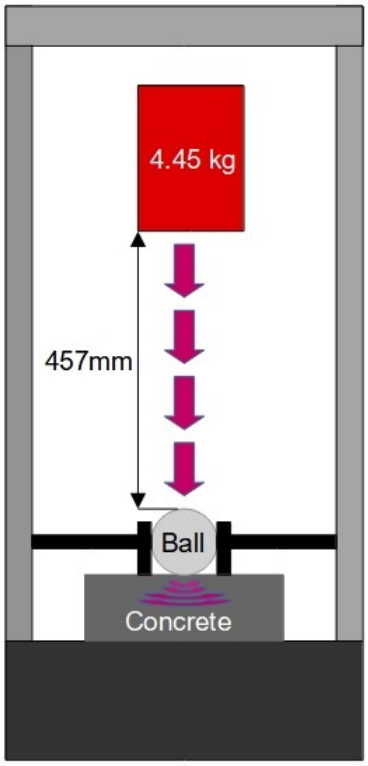


Figure 12. General view of the «Impact Resistance» test rig.

4.3.3. Frost Resistance of the Samples

The frost resistance of the samples was determined using a specialised testing system for assessing the frost resistance of concrete—«Beton-Moroz» (manufactured by «Interpribor», Almaty, Kazakhstan). Operating conditions: ambient temperature: electronic unit—from +10 to +35 °C; measuring chamber—from −20 to +35 °C; relative humidity at +35 °C and below, without condensation, up to 75%, atmospheric pressure 84–106.7 kPa [39]. The frost resistance of the concrete was assessed after a curing period of 28 days.

4.3.4. Modelling and Optimisation of Concrete Mixtures Containing ABS Plastic and Fullerene Using Response Surface Methodology (RSM)

To investigate the effect of the content of ABS plastic (X_1) and fullerene (X_2) on the strength properties, impact strength, and freeze–thaw resistance of concrete (Y), the response surface methodology (RSM) was applied. The mathematical model was represented as a full second-order polynomial (7):

$$Y = \beta_0 + \beta_1 \cdot X_1 + \beta_2 \cdot X_2 + \beta_{12} \cdot X_1 \cdot X_2 + \beta_{11} \cdot X_1^2 + \beta_{22} \cdot X_2^2 \quad (7)$$

where:

Y—design compressive strength (MPa);

X_1—factor of ABS plastic content (%);
X_2—Fullerene content factor (%);
β_0, β_1, β_2—regression coefficients.

The unknown regression coefficients β_0, β_1, and β_2 of the polynomial equation were determined using the classical least squares method (LSM). Matrix calculations were performed in a software environment using linear regression algorithms that minimise the sum of the squares of the residuals between the experimental response values and the model predictions. The model's adequacy was assessed using the coefficient of determination (R^2) and Fisher's criterion. The mean approximation error ($\bar{A}$), reflecting the average relative deviation of the calculated values of concrete properties from the actual experimental data, was calculated using Formula (8):

$$\bar{A} = \frac{1}{n}\sum_{i=1}^{n}\left|\frac{Y_{exp} - Y_{calc}}{Y_{exp}}\right| \times 100\% \quad (8)$$

where:

n—the total number of experimental data points in the database;
Y_{exp}—actual strength value obtained during laboratory testing (MPa);
Y_{calc} —calculated strength value obtained using a polynomial regression equation (MPa).

4.3.5. A Method for Evaluating the Resulting Polynomial Models Using Machine Learning Algorithms

A database for training and testing models for predicting the strength of concrete, compiled from 36 sets of laboratory tests on concrete mixes aged 7 and 28 days (72 sets in total). A database for training and testing models for predicting the impact strength of concrete, compiled on the basis of 36 series of laboratory tests on concrete mixes aged 28 days. A database for training and testing models for predicting the frost resistance of concrete, compiled on the basis of 24 series of laboratory tests for concrete mixes aged 28 days. Input parameters (X): ABS plastic content (X_1, 0–50% by mass of sand) and fullerene concentration (X_2, 0–0.020% by mass of water). Output parameter (Y): compressive strength at 7 and 28 days (R_7; R_{28}, MPa), impact strength (J_f, J) and frost resistance N (number of cycles) at 28 days. Prior to the calculations, the data was normalised using Formula (9):

$$X_{\text{norm}} = \frac{X - X_{min}}{X_{max} - X_{min}} \quad (9)$$

where X is the initial value of the factor, and X_{min} and X_{max} are the minimum and maximum values of the corresponding factor in the sample. This is necessary to ensure the stable convergence of AI algorithms.

The content of ABS (up to 50%) and fullerene (up to 0.020%) in the concrete mixture results in a comparable range of [0, 1], preventing one feature from dominating the other during the model training process.

A comparison was then carried out between three types of predictive models:

- Polynomial regression (RSM): a classical second-order model obtained using the response surface method;
- Adaptive Boosting (AdaBoost): an ensemble algorithm. This method demonstrated the highest accuracy (R^2 = 0.98) in studies of concrete compositions [24]. The method is based on the iterative construction of a composition of 'weak' algorithms–decision trees (Freund, Schapire, 1997) [40].

Random Forest. An algorithm based on the construction of a set of independent decision trees. This method was chosen due to its high resistance to overfitting when working with relatively small data samples [41].

Plots comparing the experimental and calculated values for the RSM, RF and AdaBoost models were generated using AI (Gemini AI model (Google, 2026)).

Given the limited size of the experimental sample, k-fold cross-validation (with k = 5) was used to assess the models' generalisation ability. The following statistical criteria were used to quantitatively assess the accuracy of the predictions:

- Coefficient of determination (R^2): a measure of how well the model fits the experimental data;
- Mean absolute error (MAE) [42]: reflects the average deviation of the forecast in MPa (10);

$$MAE = \frac{1}{n}\sum_{i=1}^{n}\left|y_i - y_i^p\right| \quad (10)$$

where:

n—the total amount of experimental data;
y_i—actual strength value (MPa),
y_i^p—predicted strength value (MPa).

- Root mean square error (RMSE) [43]: used to assess the sensitivity of models to significant deviations (outliers) (11);

$$RMSE = \sqrt{\frac{1}{n}\sum_{i=1}^{n}\left(y_i - y_i^p\right)^2} \quad (11)$$

where

n—the total amount of experimental data;
y_i—actual strength value (MPa);
y_i^p—predicted strength value (MPa).

4.3.6. Multi-Objective Optimisation Methods

The optimal composition of modified concrete, with an optimal combination of properties, was determined using Desirability Function Analysis. The multi-criteria optimisation tasks and the search for the global maximum of the generalised desirability function (D) were carried out using AI (Gemini AI model (Google, 2026)). The following response parameters were selected: compressive strength (R), impact strength (J_f) and frost resistance index (N). The optimisation procedure comprised the following stages:

- For each response parameter, second-order regression equations were obtained using the response surface method (RSM) to describe the influence of the ABS plastic content (P) and the fullerene dosage (F).
- As the selected parameters have different units of measurement (MPa, J, cycles), a normalisation procedure was carried out. Each value was assigned a dimensionless desirability index (di) ranging from 0 (worst value) to 1 (ideal result).

The generalised desirability function (D) was calculated as the geometric mean (or weighted arithmetic mean) of the individual response functions [44] (12):

$$D = \sqrt[n]{d_1 \cdot d_2 \cdot \ldots \cdot d_n} \quad (12)$$

By analysing the response curve D = f (P, F), the point of maximum is identified, corresponding to the most balanced mix design that ensures high performance properties of the concrete at the specified additive concentrations.

5. Conclusions

At present, plastic is regarded as a problematic filler [45,46], suitable for use at a maximum of 15–20% by weight, and only for non-load-bearing structures. Concrete modified with plastic and fullerenol, combined with the modelling of concrete properties using AI methods, offers a fresh perspective on this issue. Thanks to the introduction of fullerenol, even with a 50% content of ABS plastic, strength increases by 65% (to 26.97 MPa) and impact strength more than doubles (223.15 J for 50% plastic and 0.005% F) compared to unmodified concrete.

In classical studies, these relationships are often described linearly or using simple empirical formulas. The use of ensemble methods (Random Forest and AdaBoost) offers significant advantages:

- They effectively capture ($R^2 > 0.99$) the onset of nanoparticle agglomeration, which the classical RSM 'smooths out'. This is critically important for determining the 'saturation limit';
- Confirm that deviations in strength are not random experimental errors, but a consequence of the complex multiphase nature of the system with plastic;
- Clearly demonstrate the negative impact of excess nano-additive on strength, coefficient = $-17{,}049.2\ X_2^2$ (2), and impact toughness, coefficient = $-64{,}832.2255\ X_2^2$ (3).

It has been established that the 15% plastic limit cited in the literature applies only to systems that do not use fullerene. The use of fullerene in conjunction with AI-based analytical tools makes it possible to produce eco-friendly concrete with a high waste content (30% or more), whilst maintaining structural properties and high impact strength.

From an environmental perspective, incorporating plastic waste at a rate of 30–50% of the aggregate mass can reduce the carbon footprint (CO_2) of concrete by 6–40% by decreasing the demand for virgin raw materials and lowering overall energy consumption throughout the supply chain [47,48]. From an economic standpoint, despite the inclusion of a nanomodifier (fullerenol) in the composition, the direct replacement of raw material components with secondary ABS plastic (whose cost on the recycling market is on average 40–50% lower than that of primary aggregates or special binders) reduces the net production cost of 1 m^3 of modified concrete by 15–20% [49]. Thus, the developed method transforms plastic waste from the category of "problematic aggregates" into a highly effective resource for carbon-neutral and commercially viable construction.

Author Contributions: Conceptualization, N.A.K., R.S. and N.C.; methodology, N.A.K. and R.S.; N.C. and M.A.S.; validation, O.V.R., M.A.S. and Z.S.; formal analysis, O.V.R., M.A.S., N.C. and Z.S.; investigation, N.C., O.V.R., N.A.K., M.A.S. and R.S.; resources, N.C. and N.A.K.; visualisation, R.S.; data curation, O.V.R., Y.R. and Z.S.; writing—original draft preparation, N.A.K., R.S. and Z.S.; writing—review and editing, N.A.K., R.S. and Z.S.; supervision, N.A.K.; project administration, N.A.K.; funding acquisition, N.A.K. All authors have read and agreed to the published version of the manuscript.

Funding: This research is funded by the Committee of Science of the Ministry of Science and Higher Education of the Republic of Kazakhstan (Grant No AP23488821 «Development of a reagentless energy and resource saving technology for the extraction of non-ferrous metals from electronic waste».

Data Availability Statement: The data presented in this study are available on request from the corresponding author.

Conflicts of Interest: The authors declare no conflicts of interest.

References

1. Baldé, C.P.; Kuehr, R.; Yamamoto, T.; McDonald, R.; D'Angelo, E.; Althaf, S.; Bel, G.; Deubzer, O.; Fernandez-Cubillo, E.; Forti, V.; et al. *The Global E-Waste Monitor 2024*; International Telecommunication Union (ITU) and United Nations Institute for Training and Research (UNITAR): Geneva/Bonn, Switzerland, 2024; 145p, Available online: https://www.itu.int/en/mediacentre/Pages/PR-2024-03-20-e-waste-recycling.aspx (accessed on 7 November 2024).
2. Jain, M.; Kumar, D.; Chaudhary, J.; Kumar, S.; Sharma, S.; Verma, A.S. Review on E-waste management and its impact on the environment and Society. *Waste Manag. Bull.* **2023**, *1*, 34–44. [CrossRef]
3. Sahajwalla, V.; Gaikwad, V. The present and future of e-waste plastics recycling. *Curr. Opin. Green Sustain. Chem.* **2018**, *13*, 102–107. [CrossRef]
4. Nayanathara Thathsarani Pilapitiya, P.G.C.; Ratnayake, A.S. The world of plastic waste: A review. *Clean. Mater.* **2024**, *11*, 100220. [CrossRef]
5. Shah, H.H.; Amin, M.; Iqbal, A.; Nadeem, I.; Kalin, M.; Soomar, A.M.; Galal, A.M. A review on gasification and pyrolysis of waste plastics. *Front. Chem.* **2023**, *10*, 960894. [CrossRef]
6. Prata, J.C. The Environmental Impact of E-Waste Microplastics: A Systematic Review and Analysis Based on the Driver–Pressure–State–Impact–Response (DPSIR) Framework. *Environments* **2024**, *11*, 30. [CrossRef]
7. Chaine, C.; Hursthouse, A.S.; McLean, B.; McLellan, I.; McMahon, B.; McNulty, J.; Miller, J.; Viza, E. Recycling Plastics from WEEE: A Review. *Int. J. Environ. Res. Public Health* **2022**, *19*, 766. [CrossRef]
8. Chai, B.; Wei, Q.; She, Y.; Lu, G.; Dang, Z.; Yin, H. Soil Microplastic Pollution in an E-Waste Dismantling Zone of China. *Waste Manag.* **2020**, *118*, 291–301. [CrossRef]
9. Ferreira-Filipe, D.A.; Hursthouse, A.; Duarte, A.C.; Rocha-Santos, T.; Patrício Silva, A.L. E-Waste Plastics in the Environment: Assessment, Characterisation, and Bioprocessing. *Appl. Sci.* **2025**, *15*, 2122. [CrossRef]
10. Kaur, G.; Pavia, S. Physical properties and microstructure of plastic aggregate mortars made with acrylonitrile-butadiene-styrene (ABS), polycarbonate (PC), polyoxymethylene (POM) and ABS/PC blend waste. *J. Build. Eng.* **2020**, *31*, 101341. [CrossRef]
11. Martinho, G.; Pires, A.; Saraiva, L.; Ribeiro, R. Composition of plastics from waste electrical and electronic equipment (WEEE) by direct sampling. *Waste Manag.* **2012**, *32*, 1213–1217. [CrossRef] [PubMed]
12. Askar, M.K.; Al-Kamaki, Y.S.S.; Hassan, A. Utilizing Polyethylene Terephthalate PET in Concrete: A Review. *Polymers* **2023**, *15*, 3320. [CrossRef]
13. Tamrin; Nurdiana, J. The Effect of Recycled HDPE Plastic Additions on Concrete Performance. *Recycling* **2021**, *6*, 18. [CrossRef]
14. Al-Noaimat, Y.A.; Sambucci, M.; Chougan, M.; El-Seidy, E.; Biblioteca, I.; Valente, M.; Tirillò, J.; Al-Kheetan, M.J.; Ghaffar, S.H. Sustainable repurposing of polyvinyl chloride waste as aggregates in limestone-calcined clay cement. *J. Clean. Prod.* **2025**, *491*, 144862. [CrossRef]
15. Sanchez Soloaga, I.; Oshiro, A.; Positieri, M. The use of recycled plastic in concrete: An alternative to reduce the ecological footprint. *Rev. Constr.* **2014**, *13*, 20–26. [CrossRef]
16. Acuña-Pizano, H.; González-Trevizo, M.E.; Luna-León, A.; Martínez-Torres, K.E.; Fernández-Melchor, F. Plastic composites as sustainable building materials: A thermal and mechanical exploration. *Constr. Build. Mater.* **2022**, *344*, 128083. [CrossRef]
17. Saikia, N.; de Brito, J. Mechanical properties and abrasion behaviour of concrete containing shredded PET bottle waste as a partial substitution of natural aggregate. *Constr. Build. Mater.* **2014**, *52*, 236–244. [CrossRef]
18. Al-Akhras, N.; Sezen, H. Properties of Concrete Influenced by Plastic Materials. *Buildings* **2025**, *15*, 4061. [CrossRef]
19. Wu, J.; Yang, S.; Williamson, M.; Wong, H.S.; Bhudia, T.; Pu, H.; Yin, Q.; Ma, D.; Chen, W. Microscopic mechanism of cellulose nanofibers modified cemented gangue backfill materials. *Adv. Compos. Hybrid Mater.* **2025**, *8*, 177. [CrossRef]
20. Yang, Q.; Yang, Q.; Peng, X.; Xia, K.; Xu, B. A Review of the Effects of Nanomaterials on the Properties of Concrete. *Buildings* **2025**, *15*, 2363. [CrossRef]
21. Bautista-Gutierrez, K.P.; Herrera-May, A.L.; Santamaría-López, J.M.; Honorato-Moreno, A.; Zamora-Castro, S.A. Recent Progress in Nanomaterials for Modern Concrete Infrastructure: Advantages and Challenges. *Materials* **2019**, *12*, 3548. [CrossRef]
22. Saleem, H.; Zaidi, S.J.; Alnuaimi, N.A. Recent Advancements in the Nanomaterial Application in Concrete and Its Ecological Impact. *Materials* **2021**, *14*, 6387. [CrossRef] [PubMed]
23. Box, G.E.P.; Draper, N.R. *Response Surfaces, Mixtures, and Ridge Analyses*; Wiley: Hoboken, NJ, USA, 2007; p. 649. Available online: https://onlinelibrary.wiley.com/doi/book/10.1002/0470072768 (accessed on 3 May 2026).
24. Feng, D.-C.; Liu, Z.-T.; Wang, X.-D.; Chen, Y.; Chang, J.-Q.; Wei, D.-F.; Jiang, Z.-M. Machine learning-based compressive strength prediction for concrete: An adaptive boosting approach. *Constr. Build. Mater.* **2020**, *230*, 117000. [CrossRef]
25. Guendouz, M.; Debieb, F.; Boukendakdji, O.; Kadri, E.H.; Bentchikou, M.; Soualhi, H. Use of plastic waste in sand concrete. *J. Mater. Environ. Sci.* **2016**, *7*, 382–389.
26. Yao, S.; Yuan, X.; Jiang, L.; Xiong, T.; Zhang, J. Recent Progress on Fullerene-Based Materials: Synthesis, Properties, Modifications, and Photocatalytic Applications. *Materials* **2020**, *13*, 2924. [CrossRef]

27. Kyzyma, O.A.; Avdeev, M.V.; Bolshakova, O.I.; Melentev, P.; Sarantseva, S.V.; Ivankov, O.I.; Korobov, M.V.; Mikheev, I.V.; Tropin, T.V.; Kubovcikova, M.; et al. State of Aggregation and Toxicity of Aqueous Fullerene Solutions. *Appl. Surf. Sci.* **2019**, *483*, 69–75. [CrossRef]
28. Semenov, K.N.; Charykov, N.A.; Postnov, V.N.; Sharoyko, V.V.; Vorotyntsev, I.V.; Galagudza, M.M.; Murin, I.V. Fullerenols: Physicochemical properties and applications. *Prog. Solid State Chem.* **2016**, *44*, 59–74. [CrossRef]
29. *ASTM C33/C33M-24*; Standard Specification for Concrete Aggregates. ASTM International: West Conshohocken, PA, USA, 2024. Available online: https://store.astm.org/c0033_c0033m-24a.html.
30. Cayanan, F.; Dela Cruz, O.G.; Bornales, A.P.; Domalaon, R.M.; Marbella, J.B. A Review of the Effect of Mixing Water Quality on Concrete. In *Proceedings of the International Conference on Geosynthetics and Environmental Engineering*; Jeon, H.Y., Ed.; Lecture Notes in Civil Engineering; Springer: Singapore, 2024; Volume 374, pp. 119–128. [CrossRef]
31. *EN 1008:2002*; Mixing Water for Concrete—Specification for Sampling, Testing and Assessing the Suitability of Water, Including Water Recovered from Processes in the Concrete Industry, as Mixing Water for Concrete. British Standards Institution: London, UK, 2002.
32. Abduallah, R.; Castro, J.; Sezen, H.; Burris, L. Structural Performance of Reinforced Concrete Affected by Plastic Materials. *Buildings* **2026**, *16*, 229. [CrossRef]
33. *EN 12390-2:2009*; NEQ. Testing Hardened Concrete—Part 2: Making and Curing Specimens for Strength Tests. The European Committee for Standardization (CEN): Brussels, Belgium, 2009.
34. Rudenko, O.V.; Charykov, N.A.; Kulenova, N.A.; Sadenova, M.A.; Anop, D.K.; Kuldeyev, E. Aerated Concrete, Based on the Ash of Thermal Power Plants, Nanostructured with Water-Soluble Fullerenols. *Processes* **2024**, *12*, 2139. [CrossRef]
35. *EN 12390-3:2019*; Testing Hardened Concrete—Part 3: Compressive Strength of Test Specimens. The European Committee for Standardization (CEN): Brussels, Belgium, 2019.
36. *ACI 544.2R-89*; Measurement of Properties of Fiber Reinforced Concrete. American Concrete Institute: Farmington Hills, MI, USA, 1999; Volume 89, pp. 1–12.
37. Abid, S.R.; Abbass, A.A.; Murali, G.; Al-Sarray, M.L.J.; Nader, I.A.; Ali, S.H. Post-High-Temperature Exposure Repeated Impact Response of Steel-Fiber-Reinforced Concrete. *Buildings* **2022**, *12*, 1364. [CrossRef]
38. Bazarkhankyzy, A.; Murali, G.; Aibuldinov, Y.; Iskakova, Z.; Kurpińska, M.; Abdelgader, H.S.; Avudaiappan, S.; Dixit, S. Comprehensive evaluation of impact strength and microstructural characteristics of geopolymer concrete reinforced with four types of natural fibers of varying lengths. *Sci. Rep.* **2025**, *15*, 29624. [CrossRef]
39. *ASTM C666/C666M*; Standard Test Method for Resistance of Concrete to Rapid Freezing and Thawing. ASTM International: West Conshohocken, PN, USA, 2008.
40. Freund, Y.; Schapire, R.E. A Decision-Theoretic Generalization of On-Line Learning and an Application to Boosting. *J. Comput. Syst. Sci.* **1997**, *55*, 119–139. [CrossRef]
41. Breiman, L. Random Forests. *Mach. Learn.* **2001**, *45*, 5–32. [CrossRef]
42. Willmott, C.J.; Matsuura, K. Advantages of the mean absolute error (MAE) over the root mean square error (RMSE) in assessing average model performance. *Clim. Res.* **2005**, *30*, 79–82. [CrossRef]
43. Derringer, G.; Suich, R. Simultaneous Optimization of Several Response Variables. *J. Qual. Technol.* **1980**, *12*, 214–219. [CrossRef]
44. Chai, T.; Draxler, R.R. Root mean square error (RMSE) or mean absolute error (MAE)?—Arguments against avoiding RMSE in the literature. *Geosci. Model Dev.* **2014**, *7*, 1247–1250. [CrossRef]
45. Habib, M.Z.; Alom, M.M.; Hoque, M.M. Concrete production using recycled waste plastic as aggregate. *J. Civ. Eng. (IEB)* **2017**, *45*, 11–17.
46. Almeshal, I.; Tayeh, B.A.; Alyousef, R.; Alabduljabbar, H.; Mohamed, A.M. Eco-friendly concrete containing recycled plastic as partial replacement for sand. *J. Mater. Res. Technol.* **2020**, *9*, 4631–4643. [CrossRef]
47. Turner, L.K.; Collins, F.G. Carbon dioxide equivalent (CO_2) emissions: A comparison between geopolymer and ordinary Portland cement concrete. *Constr. Build. Mater.* **2013**, *43*, 125–130. [CrossRef]
48. Pizoń, J.; Poranek, N.; Horňáková, M. Life Cycle Assessment of Concrete Containing Crushed Concrete Paving Blocks as a Sustainable Replacement for Natural Aggregates. *Sustainability* **2026**, *18*, 2703. [CrossRef]
49. Siddique, R.; Khatib, J.; Kaur, I. Use of recycled plastic in concrete: A review. *Waste Manag.* **2008**, *28*, 1835–1852. [CrossRef]

Disclaimer/Publisher's Note: The statements, opinions and data contained in all publications are solely those of the individual author(s) and contributor(s) and not of MDPI and/or the editor(s). MDPI and/or the editor(s) disclaim responsibility for any injury to people or property resulting from any ideas, methods, instructions or products referred to in the content.